

# 1070

# Technical Challenges and Recent Developments in Underwater Imaging

Frank M. Caimi

Department of Electrical Engineering/Engineering Division  
Harbor Branch Oceanographic Institution, Inc.  
5600 US 1 North  
Ft. Pierce, Florida 34946

## ABSTRACT

The need for improved vision in various undersea applications has been recognized for decades. Improvements in underwater cameras and lenses have followed similar improvements in land-based cameras, but limitations associated with the image transfer characteristics of the medium have been primary obstacles in developing high performance systems. The application of lasers to the imaging formation process has provided a means of acquiring long range images and has, at least partially, formed the basis for the development of high power blue-green laser technology. Unlike atmospheric applications, underwater images can be formed only over small distances--perhaps only tens of meters. Distance is primarily determined by the optical power available, the system geometry, the detection means, and (primarily by) the optical attenuation of the medium. The attenuation is governed by absorption and scattering processes which act to either remove or redirect photons originating from the source of illumination. In spite of the limitations imposed by these effects, considerable progress has been made over the past several years toward increasing the image formation range and image quality. These gains have been made through the use of nonconventional image formation techniques and laser technology. This paper will review the classically described methodologies for underwater image formation, as well as their limitations, and will discuss recent developments that extend imaging capability beyond the construction of 2-dimensional reflectance maps.

For example, a system under development produces three-dimensional maps of the image space using a scanning laser configuration. The scene is viewed from a separate location to provide depth information via triangulation. The detector provides an estimate of position of the apparent landing spot of the laser beam for each scan angle from which a depth estimate is calculated. The system is designed to scan a 20 X 20 degree field-of-view at distances from 0.5 to 1.5 meters with a resolution of about 1 millimeter.

## 1. INTRODUCTION

Applications requiring improved image quality and visual information include the inspection of undersea structures, such as drilling platforms, military systems, ship hulls, cables, pipes, etc., repair tasks or activities that require the positioning of manipulators or tool pieces, biological and geological monitoring activities associated with scientific research and environmental impact studies, as well as military surveillance, identification, and detection. Although conventional cameras, including disparity stereo imaging systems, can provide a means for visualization of the work environment, they are limited by poor visibility and do not yet provide the capability for real-time quantitative measurements. Consequently, engineering research is being conducted to develop alternate methods by which meaningful two- and three-dimensional images can be formed. Principles associated with contrast enhancement and long range image formation in strongly scattering media have been developed and applied, as well as optical schemes using lasers for the acquisition of dimensional data such as surface maps and contours. Structured illumination<sup>1</sup>, moiré<sup>2</sup>, as well as acoustic approaches using high frequency sonar<sup>3</sup> have been tried with success. Surface mapping schemes based upon machine vision approaches developed in the late seventies have been investigated and are potentially of interest for some applications. Surface mapping applications include the measurement of geological features; the determination of biological specimen size, shape, or volume; the estimation of movement or behavior characteristics of specific objects; and short-range navigation and station keeping control for robotic vehicles and platforms.

## 2. LIMITATIONS OF CONVENTIONAL IMAGING

The acquisition and formation of images in the underwater environment is governed primarily by scattering and absorption processes associated with water and associated suspended particles. Illumination is subject to absorption by water molecules and subsequent conversion to heat or other light energy. Additionally, light is scattered by molecules and particles that remain in suspension. Scattering can be described by Mie, Rayleigh, Raman, and Fraunhofer (diffraction) theories with various degrees of success, depending on the size, shape, and composition of the particles. The detailed scattering behavior associated with

This material may be protected by copyright law (Title 17 U.S. Code).

singular non-spherical and multilayer particles has been the subject of recent research and has been useful in creating models for establishing the volume scattering behavior of particle fields. A great amount of effort has been put into the description of optical scattering in hydrosols as evidenced by voluminous publications on the subject<sup>4</sup>. In seawater, the scattering tends to dominate in the forward direction, resulting in a blurring of detail at high spatial frequencies. The amount of scattered light present is determined by the volume scattering function<sup>5,6</sup>, and can be characterized by the volume scattering coefficient  $s$  and the volume absorption coefficient  $a$ . The assumed relationship of these quantities to the total attenuation coefficient is:

$$\underset{\text{measurable}}{c} = \underset{\text{absorp. coef.}}{a} + \underset{\text{scatter. cof.}}{s} \quad (1)$$

The "beam attenuation" coefficient,  $c$  is the sum of both quantities (assuming raman and fluorescent contributions are negligible) and is typically defined as the distance over which the flux in a collimated beam is observed to fall to 1/e of its initial value as measured with a detector having an infinitesimally small angular acceptance angle. The remainder of the light that is not absorbed or scattered continues in the original direction of propagation, but is diminished in strength by a nearly exponential dependence upon distance. The amount of light and its direction after reflection from the surface of the object is subject to the same processes as it travels toward the detector. Consequently, the number of photons returning from a reflective object may be greatly diminished in comparison to the number being returned via the scattering process, depending upon the distance, the scattering to absorption crosssection over the angular regions of interest, and the reflectivity of the object. Contrast in the image is reduced by backscattered light arriving at the detector from the entire illuminated volume. The detected signal, if integrated over a sufficiently long time period, can contain little information from *single* reflective image points in the scene, and consequently is usually observed as a background illuminance level that adds noncoherently to the light field originating on, or reflected from, objects in the scene. Light coming from each illuminated point on the object is subject to being spread in such a way that it appears to the observer as though it were coming from a "blur" of points on the object and can be described by a characteristic point spread function.

The relative degree of absorption, in comparison to scattering, depends upon the composition of the suspended matter and upon the types and quantity of dissolved substances. Both effects depend on optical wavelength and are characterized generically according to geographic region. The deep ocean optimally passes light in the blue-green portion of the spectrum where attenuation lengths ( $c^{-1}$ ) of 20 meters are common, while in coastal regions values of 3-5 meters are characteristic with maximums shifted toward the yellow, as indicated in Table 1.

Table 1. Beam Attenuation and Wavelengths of Maximum Transmittance for Various Water Types

Clearest water	$c = 0.05 \text{ m}^{-1}$	$\lambda_{\text{max}} = 470-480 \text{ nm}$
Oceanic water	$c = 0.1 - 0.2 \text{ m}^{-1}$	$\lambda_{\text{max}} = 490 - 510 \text{ nm}$
Coastal water	$c = 0.3 - 1 \text{ m}^{-1}$	$\lambda_{\text{max}} = 510- 550 \text{ nm}$

If the photon loss due to absorption were the only effect, cameras having low light sensitivity would produce excellent images, requiring only the ability to respond to the unscattered light field returning from the scene. Unfortunately, the light scattering process is of the same order of magnitude as the absorption and therefore has a tendency to blur detail and to direct scattered photons back into the camera at a time of arrival prior to that of the reflected, unscattered photons, thereby reducing the image contrast. The relative degree of scatter in the forward or backward directions is described by the asymmetry factor  $g$  defined by:

$$g = \int_0^{2\pi} \int_0^\pi \cos \theta [P(\theta) / 4\pi] d\Omega, \quad (2)$$

where  $P(\theta)$  is the scalar phase function and  $\theta$  is the angle with respect to the direction of propagation. The scalar phase function is related to the volume scattering coefficient  $b$  and volume scattering function  $\beta$  by:

$$P(\theta) = 4\pi\beta(\theta) / b \quad (3)$$

with  $b$  being defined as,

$$b = 2\pi \int_0^{2\pi} \beta(\theta) \sin(\theta) d\theta. \quad (4)$$

The asymmetry factor is zero for isotropic scattering, near minus one for highly backscattering media, and near one for highly forward scattering media. The relative value of  $b$  in relation to  $a$  is spectrally variant and for pure water is maximum near the absorption minimum at approximately 475 nm giving water its deep blue color. The volume scattering function is naturally of great importance in determining the apparent contrast of in-water images. Its form is approximately characterized for pure water over a limited angular range<sup>7</sup> and is very nearly that expected for Rayleigh scattering:

$$\beta_{\text{water}}(\theta) = \beta(\theta)_{90} \left[ \frac{\lambda_0}{\lambda} \right]^{4.32} [1 + 0.835 \cos^2(\theta)]. \quad (5)$$

In seawater, the function is considerably forward peaked, but still a minimum at 90 degrees. At near forward angles (milliradians or less) the scattering is described by refractive index variations existing in the medium (turbulence) and may be expressed as an rms variation in refractive index from which is estimated an expected modulation transfer function<sup>8,9</sup>.

Image contrast is governed by the relative magnitudes between the scattering function integrated over the solid angle of view in relation to the exponentially decaying direct image component that is not scattered. The result is highly dependent upon the illumination geometry, the spectral characteristics of the lighting, the ambient illumination, and in the case of artificially illuminated scenes, by the overlap regions between the illumination source and the camera field-of-view. It is generally assumed that images can be formed over one or two attenuation lengths before the image contrast becomes a limiting factor. For illustrative purposes, assume that light is emanating from a point on the surface of an object. At the camera, the illumination field will consist of the sum of two components  $E_s$  and  $E_d$ , the scattered and direct fields, respectively. These components can be approximated by:

$$E_d = e^{-cz} / z^2$$

$$E_s = \left( 2.5 - 1.5 \log_{10} \frac{2\pi}{\phi} \right) \left[ 1 + 7 \left( \frac{2\pi}{\phi} \right)^{1/2} e^{-sz} \right] \frac{I s e^{-sz}}{4\pi z} \quad (6)$$

The latter function is empirically derived<sup>6</sup> for a point source and can be evaluated as a function of  $cz$ , the attenuation length, and  $\phi$ , the full angle width of the source. As the source becomes narrow in angular extent, the scattered component is reduced, but not nearly as rapidly as the direct component with increasing range. The ratio of direct to scattered illumination is plotted in Figure 1. For a typical  $c/s$  ratio of 3, the two functions are equal at an attenuation length of about 1 for source angles of  $\pi$ . In reality, more than one point is illuminated and scatter from all other points is summed at the camera, making the situation worse than is described by Eq. 6 and Fig. 1.

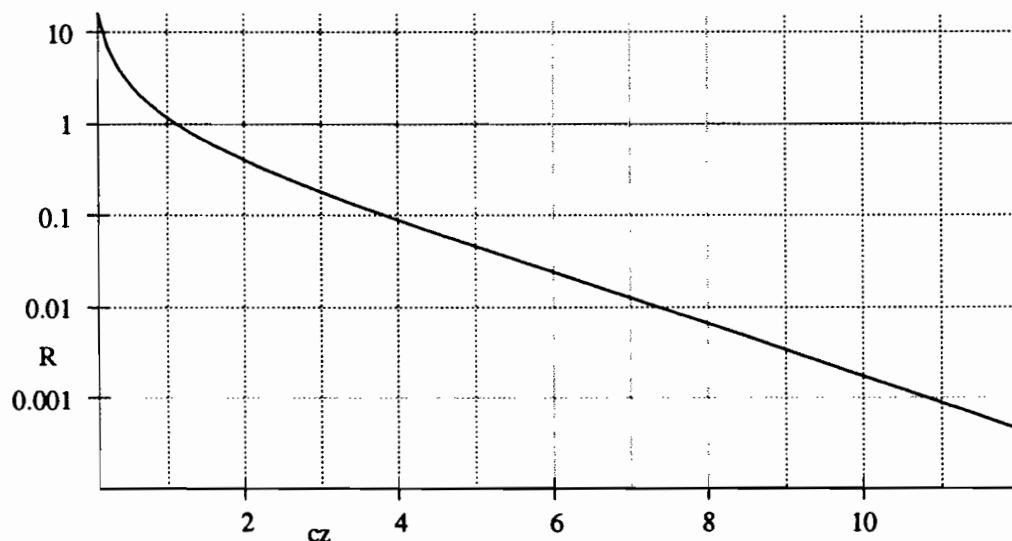


Fig. 1. The ratio  $R$  of  $E_d$  to  $E_s$  versus attenuation length  $cz$  for  $c/s = 3$ .

The primary limitation of the conventional imaging system is the loss of contrast, but the illuminance reduction is also of concern at many attenuation lengths. If the scattered field were not present, the loss would be governed by the exponentially decreasing value of  $E_s$ . At seven attenuation lengths, the illuminance is reduced by a factor of  $10^{-5}$  in comparison to the value at one attenuation length. Consequently, low light level cameras such as SIT, ISIT, ICCD, and  $I^2$ CCD are of great utility in undersea imaging applications. Since contrast limitations exist, the signal-to-noise (S/N) ratio of the camera must be optimized in order to achieve optimal information retrieval. For this reason, ICCD cameras having exceptional illuminance sensitivity but poor S/N may prove to be unacceptable in comparison to SIT types under some circumstances. Although the illuminating beam has not been expressly treated in the discussion above, it should be obvious that narrowing its angular width and reducing the field-of-view of the detector can improve the system performance substantially. It is also possible to use indirect illumination to reduce the near field backscatter by redirecting the illumination beam to allow geometric overlap at the expected maximum range<sup>10, 25</sup>. In this case it is the scattered light that is responsible for illuminating the object, rather than the direct beam. In this way, the common overlapping volume between the camera and source is minimized and contrast is enhanced.

Many of the fundamental measurements relating observed optical light fields to inherent optical properties (processes) have been conducted with support of various governmental agencies. Emphasis has been placed upon understanding the basic interrelationships of these quantities in order to gain better knowledge of the role of light in physical or chemical energy transport processes and to devise means of making remote passive color measurements for estimation of environmental parameters. The physical description of light propagation for imaging purposes has also been described Navy sponsored studies<sup>11-13</sup> and can be considered an extension of the single communication channel properties described by others<sup>14</sup>. As result of this research, unconventional methods were proposed to improve the way by which objects could be imaged. The methods incorporated laser illumination to reduce the backscatter and therefore increase image quality and range. This was accomplished in a number of ways; 1) via temporal methods using pulsed illumination and gating techniques to block scattered photons arriving at the camera prior to the arrival of photons that actually strike the object, and 2) by field limiting the detector and scanning the object or scene with a small crosssection laser beam in synchrony with the detection optics. Additional system configurations have been devised to respond to temporally encoded illumination, thereby reducing interference from background illumination or scatter. Today, variants of these systems are being produced commercially with success. This is due, in part to recent advances in solid-state lasers as well as advances in signal processing, scanning, and computer technology.

### 3. UNCONVENTIONAL IMAGING TECHNIQUES

#### 3.1 Time Gated Imaging

Time gated systems typically operate by scanning a laser beam in a point-by-point fashion over the field-of-view (FOV). A single burst of photons is produced over each element of the scan with a physical length in space that is much smaller than the beam spread at the object or smaller than any difference in photon pathlength that could originate from scatter along the direct path from laser to object and back at sufficient magnitude to compete with detection of the unscattered return beam. An example of the operation and geometric configuration of such a system is shown in Fig. 2.

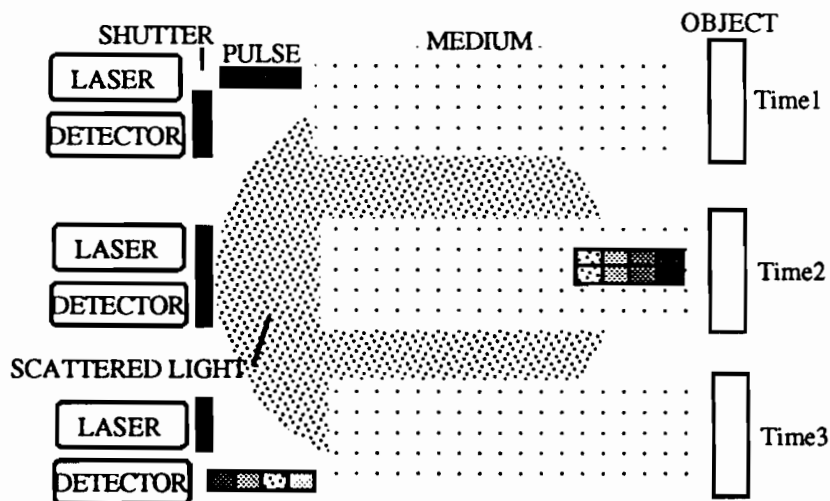


Fig. 2. Time Gating Sequence for Rejection of Scattered Light

In operation, an optical pulse is produced by the laser and is broadcast into space at an angle determined by the instantaneous position of the scan optics. The pulse is directed toward the object and is spread in time and spatial extent as it propagates. The photon packet strikes the object and is reflected according to the characteristics of the object surface. Most natural undersea objects produce diffuse reflection patterns resulting in a nearly spherical spreading loss of reflected light. The detector remains gated "off" until the photons are about to arrive at the detector aperture, thus eliminating higher intensity signal contributions from scattered photons that may arrive from nearby scattering centers. Once the detector is gated "on", a time history of the pulse is taken, and an estimate of its magnitude is recorded for display as a pixel intensity at the assumed scan location. The process is continued sequentially until the desired number of scan elements is recorded.

In water, light travels at about 4 nanoseconds per meter so that for most applications laser pulses as short as 1-5 nanoseconds are suitable. Adequate pulse energies are required to overcome absorption and scattering losses over long round trip pathlengths and to overcome detector noise for a given detector aperture. Recent advances in laser technology have improved the efficiency and reduced the size of blue-green lasers such that hand-held units are feasible, but pulse energy and efficiency is still not adequate for some applications. If the range gate is wide in comparison to the pulse, the backscattered radiance,  $B_b$ , is given as the product of  $\beta(\pi)$ , the range gate width  $dZ$ , the irradiance at the object  $E$ , and  $e^{-cZ}$ , while the target radiance is the product of the target reflectance  $\rho$ ,  $E$ , and  $e^{-cZ}$ . Thus, the contrast  $C$  is independent of range and is proportional to  $\rho$  and inversely proportional to  $\beta(\pi)$  and  $dZ$  under ideal conditions of detection.

In order to "screen" scattered light from the detector, a shutter or gating device is employed--often a gated photomultiplier tube due to its fast response and high sensitivity. The return from the detector is quantized in amplitude for each time increment allowing a 2-D reflectance image or 3-D surface map to be constructed. The 3-D information can be derived from time-of-flight information for each pulse burst. However, depth resolution at close range requires extreme temporal resolution--10 picoseconds for approximately 1 millimeter. Laser pulse rates, output energy per pulse, receiver aperture, and detector noise floor govern performance, but definite range performance improvements are possible. For instance, imaging has been demonstrated at greater than 5-6 attenuation lengths, in comparison to 1-3 attenuation lengths for conventional camera systems. A system producing images at 4-5 attenuation lengths has been demonstrated using a Nd:YLF laser at 526 nm<sup>15</sup>. This system operates in a linescan mode and requires movement to generate the second axis of the image. The laser is diode pumped and produces an 11 kW, 11 ns pulse at a pulse repetition frequency of 1 kHz. The system utilizes a 90 degree scan width and a receiver FOV of 5 mrad to produce a range accuracy of  $\pm 5$  cm.

Light Detection and Ranging (LIDAR) methods where time-of-flight information is used to obtain range estimates are typically used in airborne remote sensing and some undersea military applications. Pulse repetition rates suitable for video frame rate imaging are desirable for many applications involving relative motion between the detection platform and the scene.

Alternative time gating methods use pulsed lasers to illuminate the entire scene (or portions of the scene) at one brief window in time and can produce extended range reflectance (2-D) images. In these systems the requirement for a rapid pulse repetition rate is relaxed but the required energy per pulse is increased. Detectors commonly used with this illumination method include gated intensified cameras, such as ISIT or ICCD types. An advantage of this approach is that standard low light cameras are readily adapted without the need for special purpose scanners or detectors. A developmental system produced by Sparta, Inc. in San Diego has produced images at 5-6 attenuation lengths<sup>16</sup>. A Q-switched Nd:YAG laser doubled to 532 nm was used at a pulse energy of 100 mJ at a repetition rate of 30 Hz. The laser efficiency is approximately 1%, resulting in a total power consumption of less than 500 Watts. Similar systems are planned for incorporation into various undersea platforms over the next several years.

### 3.2 Field limited imaging

Another method for the reduction of scattered light effects on the image involves the synchronous scanning of a narrow laser beam with a narrow field-of-view detector.

In this case, the scattered light returned to the detector is reduced by minimizing the overlap between the illuminated volume and the detector field-of-view and placing the overlap region closer to the object in the scene, as shown in Fig. 3. This process is analogous to following the light from a laser pointer with a telescope, and assumes some knowledge about the distance to the surface. Several "synchronous scan" systems are being marketed commercially by Applied Remote Technologies and formerly by Westinghouse Laser Systems in San Diego. Demonstrated performance is approximately 5 attenuation lengths<sup>17</sup>. Detailed comparison studies between the field limited and time gated systems have been conducted<sup>18</sup>.

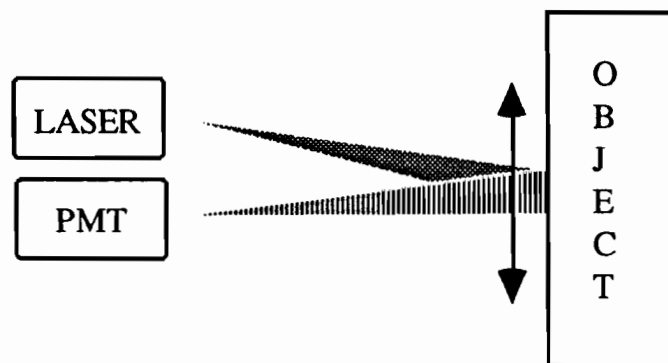


Fig. 3. Synchronous Scan Geometry

#### 4. EXTENDED CAPABILITY IMAGING SYSTEMS

##### **4.1 Image gradient systems**

Undersea images often exhibit nearly identical reflectance over a two-dimensional cross section. This condition is worsened by the contrast reduction caused by particulate scattering, making the identification of key features on the object surface a difficult task, especially with lighting that can be nonuniform and contain artifacts. For applications such as pipe inspection or structural inspection, it is desirable to obtain additional information relating to the object contour or depth profile. Standard video or still cameras are not able to obtain this information directly, although methods using optical flow and image gradients have been applied to obtain shape, velocity, and position information using intensity gradients observed in the scene as a result of illumination from natural or artificial light sources<sup>19,20</sup>. Many of these methods have been demonstrated in research laboratories but remaining problems include the requirement for optical modeling of the medium effects upon shape-from-shading and optical flow methods.

##### **4.2 Structured illumination systems**

Several undersea inspection systems have been developed using laser structured illumination for producing 3-dimensional data<sup>21</sup>. These systems operate in either a fly-by or slow scan mode and rely upon spatial disparity of the laser projector and sensor to determine range by triangulation. "Fly-by" systems typically use a single laser stripe projection to scan broadside to the vehicle motion in order to produce a series of one-dimensional range maps which can be analyzed as the scan crosses the object under inspection. By contrast, "scan mode" systems employ a high resolution 2-D laser scanner in addition to a high resolution position sensitive detector, such as a 1-D CCD array to detect the laser reflection at every point of the scan. A two-dimensional range map is produced, but at a slow rate sometimes taking minutes.

A high speed system (SUMS) was developed at Harbor Branch Oceanographic Institution under contract to the Naval Civil Engineering Laboratory<sup>22</sup>. The system produces 3-D maps of unhidden surfaces within a 40° field-of-view at a relatively short range of 1-2 meters in a period of less than 5 seconds. The apparent position of the laser reflection against the scene is determined with an accuracy of better than 1 part in 1000, providing similar resolution to distinguish differences in range to each point in the scan. Each scan generates a two-dimensional matrix of range values that when taken as a whole provides a three-dimensional relief map of the area of interest. The relief map can then be rotated and viewed from different angles and distances by the operator. The operator is also able to control the extent, positioning, speed, and resolution of the laser scan anywhere within the field-of-view. The system is capable of detecting features occupying an angular field of 0.05 degrees (approximately 200x200 pixels) or greater (800 x 800 pixels) while distinguishing differences in range over the scanned volume of less than 1 mm at a standoff distance of 1000 mm.

##### **4.3 SUMS system description**

The system is configured to raster scan a region of space using a frequency doubled Nd:YAG laser. Return light from the laser scanner is received at an adjacent location. The received light is focused onto a position sensitive detector (PSD) which produces an estimate of the reflected beam location, from which the range coordinate of the surface may be computed by triangulation. A diagram of the system geometry is shown in Fig. 4.

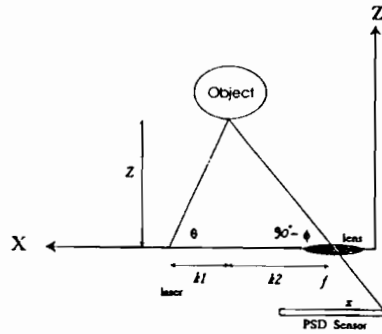


Fig. 4. Configuration of a flying spot laser scanner system (SUMS) used for underwater surface mapping.

The system was designed to map surface features at close range, approximately 0.5-2 meters, with a positional accuracy of 1 millimeter with optical beam attenuation coefficients as large as  $0.5 \text{ m}^{-1}$ . In clear water, the system forms reasonably accurate representations of highly reflective surfaces, such as the one shown in Fig. 5. This image of a dome and stepped wedge object was taken in a test tank environment at a nominal range of 1 meter. Under these conditions, the system performance is primarily limited by the laser power available (150 mW), the detector aperture size, and by the detector signal-to-noise ratio, limiting the useful range and scan rate to approximately 2 m and 10 kHz/voxel, respectively.

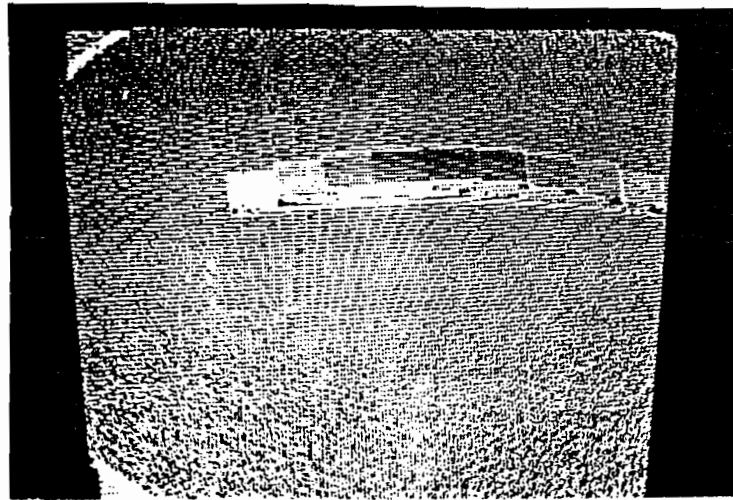


Fig. 5. Test tank 3-D image reconstruction of stepped-wedge object (steps 1 to 4 mm) at 1 m nominal range. ( $c = 0.05 \text{ m}^{-1}$ ).

In turbid water, however, tests have indicated some inherent distortion arising from scattered light that enters the detector aperture, resulting from a skewing of the response function of the position sensitive detector away from the reflected light centroid<sup>23</sup>.

#### 4.4 SUMS Triangulation theory

The system geometry is shown in Fig. 4. We assume that the laser is scanned through angles  $\theta_x$  and  $\theta_y$  and that the separation of the laser scan center and detector axis is BL. The detector produces a measure of the reflected light position along the x-axis in the image plane. The z-axis position can be estimated from:

$$Z(t) = \frac{BL}{\frac{x(t)}{f} + \frac{1}{\tan \theta(t)}}, \quad (7)$$

$$X(t) = Z(t) \frac{x(t)}{f} = Z(t) \tan \varphi$$

where  $f$  is the equivalent focal length of the lens forming an image at the detector,  $BL$  is the baseline length, and  $\theta$  is the horizontal projection angle, which are known quantities. Capital and lower case symbols are referred to the object and image plane coordinate systems, respectively. In order to determine the magnitude of the  $z$ -coordinate, accurate estimates for  $x$  and  $\theta$  should be obtained. Although  $\theta(t)$  may be easily derived from the scanner, estimates of  $x(t)$  are subject to errors from noise from the detector and scan geometry.

The  $z$ -axis resolution is determined by the  $x$ -axis resolution,  $dx$ :

$$\frac{dx}{dz} = Kf / z^2 \quad (8)$$

Thus, the resolution is reduced in proportion to the square of the range for a given system geometry and lens focal length. As the range is increased, however, the focal length may also be increased to reduce the FOV. If  $f$  is increased in proportion to the range, the percentage change in range ( $dz/z$ ) will produce the same  $dx$  at the detector. Increases in the laser power or detector sensitivity would allow this method to be used at greater standoff distances.

#### 4.5. SUMS Position Estimation Method

It can be shown that the error in the coordinate geometry originates from side and backscatter from the beam, as well as from the scene illumination profile. The amount of scatter can be estimated from a radiometric model that is then used to develop an error function from which a revised and more accurate estimate is made. The detector provides a first estimate of the scene geometry from the computation of the  $Z$  coordinate from the  $x$  and  $y$  position estimates. This information is used to provide a basis for determining an error function, determined from a model from which an improved estimate of the centroid offset can be obtained for each coordinate triad in the image. Alterations in the  $Z$ -coordinate estimate can be made at each iteration to offset a reduction in the error function.

Therefore, to correct these turbidity effects, and to obtain a more accurate estimate for the light centroid, an iterative adaptive signal processing estimation technique has been developed<sup>24</sup>. The adaptation algorithm is designed to minimize an appropriate cost function formed by the resulting error due to the distorted measurements in the presence of the turbid conditions. Repeated scans are made in an iterative fashion to reach a desired minimum of the error function. This process improves the accuracy of the positional estimate in a fashion that is independent of the surface location, reflectivity, and size. A greater amount of time is required in the construction of the corrected image (data set) according to the number of iterations required for the desired error reduction. Algorithms for the estimation of the more accurate position of the light centroid may be implemented by a dedicated special purpose digital signal processor, based on data collected.

#### 4.6. Low power system implementation

Enhanced performance of the laser mapping system shown in Fig. 4 can be obtained through modification of the original design concept to include image amplification as shown in Fig. 6. This system is presently under development at HBOI.

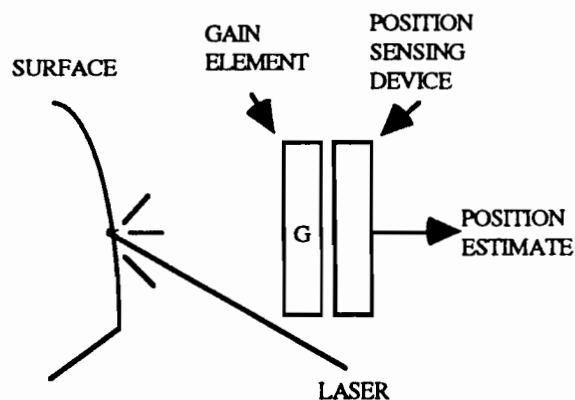


Fig. 6 Advanced Triangulation Concept



The gain  $G$  provides the ability to: increase the range  $Z$ ; to accommodate lower reflectivities  $R$ ; and to increase the scan rate because of the nature of the detection process. Assuming a detector performance comparable to the previously developed system, a gain  $G = 80$  can provide a scan rate 80 times faster without a sacrifice in resolution. Thus, a scan rate of  $1/4 \text{ sec}^{-1} \times 80 = 20 \text{ Hz}$  would be possible.

Additional gain would also provide the ability to reduce the laser power and thereby achieve portable operation, at least at close range. A practical power budget for such a system can be formed with promising results. The approximate power arriving at the detector is given by:

$$P_D = \frac{F_{det} f^2}{8 f_{\#}^2 n_w^2} \quad (9)$$

where  $f$  and  $f_{\#}$  are the focal length and f-number of the imaging lens,  $F_{det}$  is the power leaving the object surface, and  $n_w$  is the refractive index of water. A sample calculation using a laser power of 10 milliwatts and typical attenuation factors for 670 nm wavelength, provides an input light level to the gain element of approximately 1 nanowatt at a range of 1 meter distance. The required power at the position sensing device is dependent upon the background noise level at the frequency of operation. A requirement for a 20 Hz scan rate and a 200 x 200 scan resolution predicates an 800 kHz response bandwidth at the detector. Since the inherent noise level is determined by shot and thermal processes (approximately 5 nanowatts noise equivalent power), the required gain must be sufficient to overcome the noise by a sufficient margin to achieve an adequate signal-to-noise ratio. The computation of the range from Eq. 7 at a resolution commensurate with the required range resolution (1 part in 200) necessitates a gain of 1000. Our initial experiments indicate that the required gain and output power of 1 microwatt are achievable. It is noteworthy that synchronous scan and range gating techniques are applicable to this system for reduction of scattered light interference.

#### 4.7 Ambient light interference

In addition to the previously mentioned effects, light induced interference can be a dominant source of error in any low power system. There are several possibilities to eliminate as much background light as possible: 1) use the attenuation properties of water to screen ambient light by selecting a wavelength of operation that provides the desired degree of attenuation while maintaining sufficient laser signal at the detector; 2) incorporate narrowband filters at the detector aperture to pass only the laser linewidth; 3) temporally modulate the laser and synchronously detect the return; 4) reduce the angular aperture of the detector and synchronously scan, if necessary; 5) operate in deep water or at night.

Selection of laser wavelength is a particularly attractive method whereby the surrounding medium acts as an effective optical filter. Requirements for effective use of this option are to ensure that the distance from the source of interference to the detector aperture is much greater than the distance to the object. For short range applications, this condition is almost always fulfilled. The wavelength is chosen to provide an acceptable attenuation factor from the laser to the subject, while maximizing the attenuation of the surrounding medium. In seawater, the attenuation rises significantly at the infrared and ultraviolet edges of the visible spectrum. The total attenuation constant  $c$  of clean seawater is approximately  $0.4 \text{ m}^{-1}$  at 670 nm and increases to  $2 \text{ m}^{-1}$  at 800 nm. Semiconductor lasers are readily available in this wavelength range and may be selected for a particular system requirement. Operation at a 670 nm wavelength has been chosen for the initial prototype development at HBOI.

Interference from solar radiation can be reduced further by selecting a wavelength corresponding to water or other absorption lines in the solar spectrum. The downwelling irradiance in water is severely curtailed at wavelengths in excess of 600 nm; for instance, at 5 meter depth the irradiance is about  $10 \text{ nW cm}^{-2} \text{ nm}^{-1}$  in clear water, while at 25 m depth it is  $0.03 \text{ nW cm}^{-2} \text{ nm}^{-1}$ . These figures are significantly smaller in the 670 nm to 800 nm wavelength range. Thus, the use of wavelength filtering methods in conjunction with typical interference filters (FWHM = 10 nm) can limit solar interference effects to a tolerable level in comparison to the detector noise equivalent power, without resorting to temporal modulation methods, if the operating depth is sufficiently large.

Initial laboratory tests of the configuration shown in Fig. 6 have been successful using a 5 milliwatt 670 nm semiconductor laser. The results are shown in Table 2.

Table 2. Experimental Results: Optical power (670 nm) at Detector from Fig. 6.

Laser Power (mW @ 670)	Distance (m)	Power( $\mu\text{W}$ ) @ Detector
2.5	1	3.0
1	1	1.18

These results were taken with steady state optical excitation, but generally indicate the performance that can be achieved at scan rates of 800 kHz. Detector power greater than 1 microwatt is sufficient to operate the system with depth resolution greater than 1 part in 200.

## **5. INTERFEROMETRIC IMAGING**

Interferometric techniques can offer improvements in range resolution beyond that attainable from structured illumination methods and can potentially distinguish the light field returning from the scene from that generated by scattering or other effects. Although optical interferometric schemes (holography and correlation methods) have been investigated for use undersea, they rely upon the coherence of the illuminating source and intervening medium. A substantial amount of effort has been expended in this regard but system complexity and other factors have limited commercialization. An alternative to using coherency of the optical beam is to construct spatial or temporal gratings by modulation methods.

One such technique, video moiré, relies upon interference of two spatial gratings and offers an intermediate solution for resolving detail in the object contour. In the classical projection moiré system the distorted target grating is viewed through a physical reference grating. This reference grating has the effect of a binary optical filter in that opaque areas of the grating allow no information to be transmitted, while clear areas of the grating allow information to be passed. By using a special video processor this situation may be duplicated electronically. The output of the video processor circuit is an image showing equal depth moiré contours superimposed on the target.

In a collaborative effort between Florida Institute of Technology and Harbor Branch Oceanographic Institution, a moiré contouring system was demonstrated that generates real-time surface contours with zoom magnification capability. The system is particularly suited to underwater use since only one standard video camera is used in conjunction with a laser grating projector<sup>2</sup>.

The potential for using real-time video moiré techniques to distinguish between damaged and undamaged areas on structures appears to be promising for underwater inspection applications but has yet to be proven in the field in real world conditions.

## **6. SUMMARY**

In this paper, we have reviewed the basic methods used in underwater image formation and have illustrated some of the tradeoffs possible. We have also described several recent developments in undersea imaging, including a system concept that allows close range (1 m) surface mapping at video scan rates with low power semiconductor lasers. New developments will certainly utilize continuing advances in the efficiency, power output, and size of blue-green lasers and will probably take advantage of advances in narrowband, wide-aperture filter technology to reduce interference from ambient lighting. With continued improvements in laser and solid state technology, it is expected that new applications of undersea laser-based imaging technology will continue to evolve and that these will provide benefit to all aspects of marine industry and science.

## **7. ACKNOWLEDGMENTS**

The support of the U. S. Navy under contract N47408-91-C-1209 is gratefully acknowledged for initial prototype development, as well as the National Science Foundation under grant OCE-9318399 for advanced development. Additional support of the Atlantic Foundation for system development is gratefully acknowledged. We also thank Dr. Edith Widder, Dr. Anthony Bessios Dan Gravitz, David Smith, and Donna Kocak for their respective contributions to this effort. This paper is Harbor Branch Oceanographic Institution contribution number 1070.

## **8. REFERENCES**

1. Caimi, F., and R. F. Tusting, "Application of Lasers to Ocean Research and Image Recording Systems," Proc. Intl. Conf. Lasers-87, pp. 518-524, 1987.
2. Caimi, F., J. Blatt, B. Grossman, et al., "Advanced Underwater Laser Systems for Ranging, Size Estimation, and Profiling," Marine Technology Society Journal, v. 27, No. 1, pp. 31-41, 1993.
3. Jaffe, J. and P. M. Casscreau, "Multimode Imaging for Underwater Robots," Proc. SPIE v. 768, pp. 107-111, 1987

